24th ABCM International Congress of Mechanical Engineering
December 3-8, 2017, Curitiba, PR, Brazil

COBEM-2017-1813
EVALUATION OF THE CHIP SEPARATION MECHANISM DURING MACHINING OF AN AUSTENITIC STAINLESS STEEL

Gil Magno Portal Chagas
Instituto Federal de Santa Catarina, Campus Jaraguá do Sul - Rau, Rua dos Imigrantes, 445, Rau, Jaraguá do Sul - SC
gilchagas@ifsc.edu.br

Izabel Fernanda Machado
Universidade de São Paulo, Escola Politécnica, Rua Prof Mello Moraes, 2231, São Paulo - SP
machadoi@usp.br

Abstract. *The mechanisms involved in the chip formation and material separation in ductile metals is controversial. The common idea is that during machining the material is fractured and forms a new surface. Though, a crack ahead of the cutting edge has not been observed during the process. Another idea considers that the chip formation occurs with severe plastic deformation, around the cutting edge, according to a mechanism similar to an indentation, without material separation. To analyze the mechanisms involved in the chip separation of an austenitic stainless steel, a finite element simulation and experimental procedures were carried out. A quick stop device was used to obtain the chip roots for experimental observations. The machining simulation presented a severe plastic deformation near the cutting edge, and the stress state indicated a possible occurrence of chip fracture. The chip root observation indicated the evidence of ductile fracture with material separation during chip formation.*

Keywords: *machining simulation, chip formation, orthogonal cutting, austenitic stainless steel*

1. INTRODUCTION

During machining the material is subjected to high strains, high strain rates and temperatures. This condition leads to a very complex phenomenon which involves severe plastic deformation and severe friction between the tool and the workpiece. The restricted area where the chip formation occurs and the high speeds involved in the process makes it difficult to direct measure and observe.

The mechanisms involved in the chip formation and separation in ductile metals are controversial. There are two theories to explain the chip formation (Rosa, Martins and Atkins, 2007; Subbiah, Melkote, 2008). The first theory considers that there has to be a localized fracture in chip formation leading to material separation and forming a new surface. However, literature presents very few proofs of material separation by fracture in machining ductile metals. Another theory proposes that the presence of an edge radius causes a ploughing ahead of the cutting tool, similar to an indentation, and material flows around the cutting edge radius, forming the chip, without fracture and material separation (Madhavan, Chandrasekar and Farris , 2000).

Many analytical models were developed to understand and evaluate the machining process (Shaw, 2005). These models usually consider the chip formation as a result of plastic deformation and friction only. This principle is also implicit in the slip-line model, which is considered a more realistic analytical model for machining (Astakov, 2006; Arrazola et al., 2013). Atkins (2003) contested the idea of modelling metal cutting considering only deformation and friction, and concluded that the work of fracture and creation of a new surface must be considered during machining. This idea was investigated and confirmed on the works of Subbiah and Melkote (2007), and Rosa, Martins and Atkins (2007). Nevertheless, Childs (2010) investigated the chip formation considering the ploughing forces with plastic deformation and friction; he concluded that there is no need to include ductile fracture energy from forming fresh surfaces in models of continuous chip formation.

Different finite element (FEM) models were developed to simulate the machining process (Arrazola et al., 2013; Lindgren et al., 2016). However, the development of predictive models for machining is a great challenge due to the complex phenomena involved, with very large and localized deformations which may cause numerical problems with elements excessively distorted. One group of models considers that, during machining, a severe plastic flow occurs around the edge of the cutting tool and forms the chip, without fracture. This approach is used in commercial FEM softwares Deform^{TM} and Advantedge^{TM}, and requires a powerful dynamic remeshing of the elements during simulation due to the large deformation involved. Another group of models requires a chip separation criterion and can consider damage and ductile fracture that leads to material separation and the formation of a new surface. These models are commonly developed with the use of the FEM software Abaqus® and usually do not require the use of remeshing techniques.

This work uses finite element simulation considering damage and material separation to form the chip, and an experimental procedure to investigate the chip formation and separation mechanism. Based on the stress and strain obtained in the simulation and the microscope observations of the chip roots, it is possible to analyze and evaluate the mechanism involved in the chip separation of an AISI 304 and AISI 303 austenitic stainless steels.

2. NUMERICAL AND EXPERIMENTAL PROCEDURE

2.1 Numerical procedure

The orthogonal numerical simulations were conducted using the finite element software Abaqus. An elastic-plastic, explicit, plane strain, Lagrangian, fully coupled thermo-mechanical model was developed for the machining cutting process, according to Chagas and Machado (2015).

A four node plane strain quadrilateral element, CPE4RT, with automatic hourglass control and reduced integration was used for the coupled temperature displacement analysis. The workpiece, made of AISI 304 stainless steel, was 3 mm length and 0.6 mm height and was meshed with 11546 elements. The cutting tool, made of tungsten carbide, had 1.4 mm in height and 1 mm length, clearance angle α=11° and rake angle γ_0=6° was considered perfectly sharp, and modeled as rigid to reduce the calculation time and meshed with 975 elements.

The Johnson and Cook (1983) constitutive model was used in the machining simulation, and describes the flow stress of a material as the product of strain, strain rate and temperature effects as given in Eq.(1).

$$\sigma = (A + B\varepsilon^n)\left(1 + C\,ln\frac{\dot{\varepsilon}}{\dot{\varepsilon}_0}\right)\left[1 - \left(\frac{T - T_r}{T_m - T_r}\right)^m\right] \tag{1}$$

where σ is the equivalent stress, ε is the equivalent plastic strain, $\dot{\varepsilon}$ is the strain rate, $\dot{\varepsilon}_0$ is the reference strain rate, A is the initial yield stress, B is the hardening modulus, C is the strain rate coefficient, n is the strain hardening coefficient, m is the thermal softening coefficient, T is the process temperature, T_r is the room temperature, and T_m is the melting temperature of the workpiece.

The Johnson Cook (JC) parameters utilized are adopted from Lee et al. (2006), and are presented in Table 1.

Table1. Johnson Cook parameters for AISI 304

A (MPa)	B(MPa)	C	n	m	$\dot{\varepsilon}_0$
310	1000	0.07	0.65	1	1

An erosion zone was defined to allow the chip separation and reduce mesh distortion. A different criterion was utilized for the erosion zone and for the chip. The separation zone used ductile damage criterion, while the chip zone used the shear damage.

The material is assumed to have damage initiation, and its corresponding strain softening, when the damage indicator w, according to Eq. (2), reaches unity. In Equation 2 the parameter $\Delta\bar{\varepsilon}^p$ is the equivalent plastic strain increment, and $\bar{\varepsilon}_c^p$ is the equivalent plastic strain at the onset of damage (SIMULIA, 2012).

$$w = \sum \frac{\Delta\bar{\varepsilon}^p}{\bar{\varepsilon}_c^p} \tag{2}$$

Once the damage initiation criterion had been reached, it is necessary to evaluate the damage evolution, which is realized through the damage parameter D.

The chip separation zone assumes a linear damage evolution with the plastic displacement according to Eq.(3), where $\bar{u}$ is the equivalent plastic displacement, and $\bar{u}_f$ the equivalent plastic displacement at failure. The chip assumes an exponential evolution with plastic displacement given by Eq. (3).

$$D = \frac{L\bar{\varepsilon}}{\bar{u}_f} = \frac{\bar{u}}{\bar{u}_f} \tag{3}$$

The scalar damage parameter D is used to describe the degradation of the material stiffness once the initiation criterion had been reached. The material flow equivalent stress $\bar{\sigma}$ is given by Eq.(4), where $\bar{\sigma}_h$ is the hypothetical flow stress that would occur in the absence of damage. An element loses its stiffness when D = 1.

$$\bar{\sigma} = (1 - D)\bar{\sigma}_h \quad (4)$$

Figure 1illustrates the stress strain behavior of a material considering damage initiation and evolution .

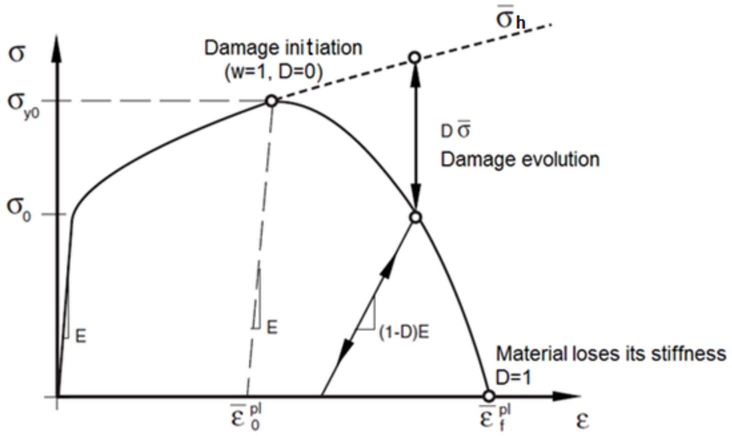

Figure 1. Stress strain curve with progressive damage (adapted from Simulia, 2012)

The tool chip contact interface was modeled according to Zorev's stick-slip contact friction model. The model considers the existence of two distinct contact regions; near the tool tip is the stick region where the shear stress, $\tau_{f,}$ is equal to the plastic yield, $\tau_{y,,}$ according to Eq.(5), and a sliding region, on the tool rake face, where a Coulomb model is adopted according to Eq.(6) (Ozel, 2006).

$$\tau_f(x) = \tau_y \text{, when } \mu\sigma_n(x) \geq \tau_y \quad (5)$$
$$\tau_f(x) = \mu\sigma_n(x)\text{, when } \mu\sigma_n(x) < \tau_y \quad (6)$$

where σ_n is the normal stress. The friction coefficient considered in the simulation was μ=0.15, and the maximum value of shear stress considered in the region was τ_f = 35 MPa.

The austenitic stainless steels AISI 304 and AISI 303 evaluated in this work are quite similar; however, AISI 303 has higher values of sulfur, to form MnS particles. According to ASM (2005) both steels have similar mechanical properties, yield stress σ_y= 205 MPa, ultimate stress σ_{ut} = 515 MPa and elongation 40%, at room temperature. Therefore, material properties and JC parameters selected for the simulations were the AISI 304 ones. Table 2 shows the chemical composition of both steels.

Table 2. Chemical composition of the austenitic stainless steels (Souza, 2006)

Material	C	Mn	Si	Cr	Ni	P	S
AISI 303	0.050	1.88	0.48	17.2	8.21	0.036	0.20
AISI 304	0.055	1.80	0.58	18.1	8.54	0.037	0.03

The workpiece and tool physical properties considered in the simulation are shown in Tab. 3.

Table 3. Workpiece and tool physical parameters (Lee et al.,2006; Agmel et al., 2011; Matweb, 2017)

Physical parameter	Workpiece AISI 304/303	Tool Tungsten carbide
Density (kg/m^3)	8000	12000
Elastic modulus, E (GPa)	210	540
Poisson's ratio, ν	0.3	0.22
Specific heat, Cp (J/KgK)	500	203
Thermal conductivity (W/mK)	16.2 (t=373K) 21.5(t=773K)	40
Thermal expansion (µm/mK)	17.3	4.7
Tmelt (K)	1673	-

The simulation used a fully coupled thermo-mechanical analysis with thermal exchange between the tool and the workpiece. It was considered 90% of the work of plastic deformation of the chip converted into heat, according to Arrazola and Ozel (2010), Rodrigues and Martins (2010), List, Sutter and Bouthiche (2012). The thermal exchange between the chip and the environment was neglected, since the process is very fast, in the order of 10^{-3} s.

2.2 Experimental procedure

Semi orthogonal and orthogonal cutting tests were carried out in a conventional lathe with dry cutting. The tool was made of tungsten carbide TPUN 160304 P30 - P40 with clearance angle α=11° and rake angle γ_0=6°.

Cutting forces tests for different cutting speeds were carried out in a conventional lathe using a piezoelectric turning dynamometer Kistler 9265B/ 9441B, signals conditioner 5070A 11100, and signal processing software DynoWare 2825A1-2.

The chip roots specimens were obtained using a quick stop device, developed according to Chern (2005) model, and were analyzed in the JEOL JSM-6010LA Scanning Electron Microscope (SEM). The tests were carried out using shafts made of AISI 304 and tubes made of AISI 303. The cutting speeds used during the tests were vc = 50 m/min, vc=79m/min and vc = 127m/min., feed rate f = 0.1mm/rev and depth of cut ap = 1mm and ap = 2mm.

3. RESULTS AND DISCUSSION

3.1 Numerical simulations results

Cutting forces obtained in the simulations were compared with those from experiments and are presented in Tab. 4. The difference between the experiments and numeric simulations were calculated, and the greater value was observed when machining with cutting speed vc=50m/min. This may be caused by the build up edge formation which was not considered in the simulation. Temperatures in the primary shear zone were compared with those obtained in an analytic procedure used in Oxley theory (Lalwani, Mehta, Jain, 2006) and presented in a previous study (Chagas and Machado, 2015).

Table 4. Numerical and experimental cutting forces (Fc), numerical and analytical temperatures in the primary shear zone (T_{PSZ}) for different cutting speeds (vc), feed rate f = 0.1mm/rev, ap = 2mm.

vc(m/min)	Fc(N) Numeric	Fc(N) Experim.	Diference Fc (%)	T_{PSZ}(°C) Numeric	T_{PSZ}(°C) Analytic
50	630	765±51	17.6	391	453
79	624	659±97	5.3	403	422
127	622	638±114	2.5	421	418

Figure 2 show some results obtained in the simulation considering vc= 79 m/min, f = 0.1mm/rev and ap = 2 mm. Figure 2(a) presents the von mises stress and Figure 2(b) the effective strain. It is possible to observe that the highest stress occurs in the primary shear zone and begin in a region near the cutting edge. The higher strains were obtained in the secondary shear zone.

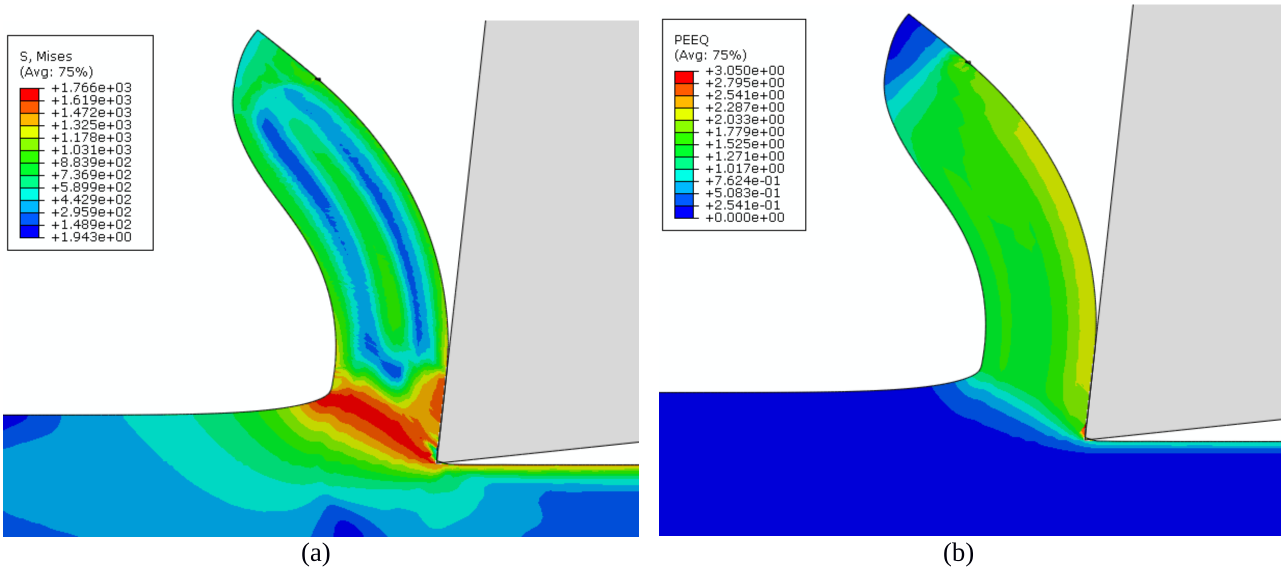

Figure 2. Simulation results: (a) Von Mises Stress [MPa]; (b) Effective strain. vc= 79 m/min, f = 0.1mm/rev and ap=2mm.

The temperatures represented in kelvin are presented in Fig. 3. The medium temperature obtained in the primary shear zone was 403°C. The higher temperature, 603°C, was obtained in the secondary shear zone due to the higher deformation and the friction between rake face of the tool and the chip.

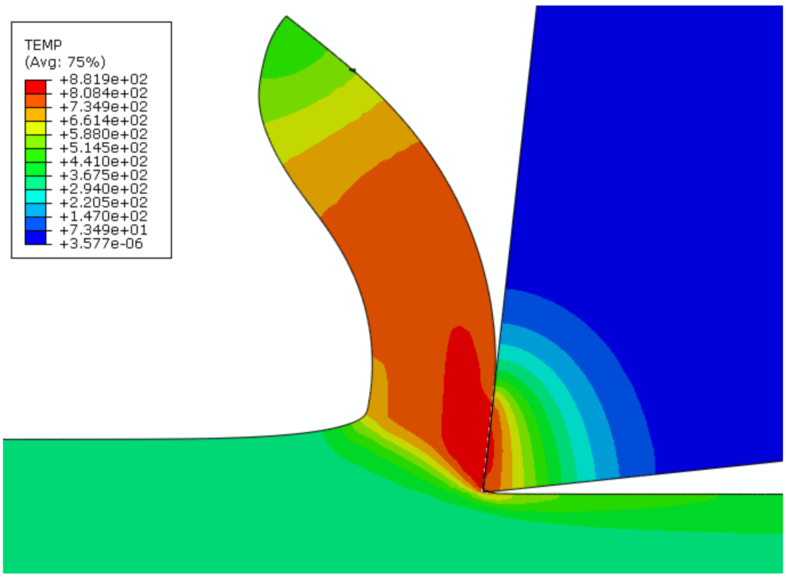

Figure 3. Temperature [K]. vc= 79 m/min, f = 0.1mm/rev and ap = 2 mm.

During the chip formation the material is under a complex state of stress with simultaneous occurrence of tensile, compressive and shear stresses in different directions. An important parameter to evaluate the chip breakage is the hydrostatic stress. Positive hydrostatic stress means the existence of normal tensile stress which favors a crack formation in ductile metals. Otherwise, negative hydrostatic stress inhibits a crack formation. The hydrostatic stress can be calculated from three principal stresses σ_1, σ_2, σ_3 according to Eq.(4).

$$\sigma_m = \frac{\sigma_1+\sigma_2+\sigma_3}{3} \tag{4}$$

Figure 4 presents the hydrostatic stresses obtained in the simulation.

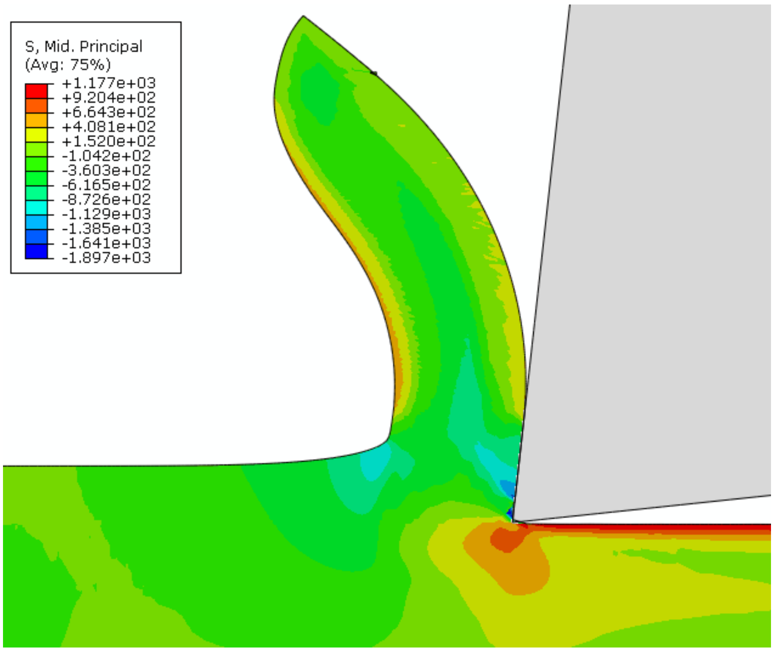

Figure 4. Hydrostatic stress [MPa]. vc= 79 m/min, f = 0.1mm/rev and ap = 2 mm.

The results show a region adjacent to the rake face of the tool with negative stresses which indicates high compression. Otherwise, the hydrostatic stresses behind the tool tip, in the workpiece, and near the rake face, represented in dark red, were positive. This tension stress is consistent with those obtained by Rosa et al. (2007) which indicated the presence of stresses of opposite sign near the tool tip. These stresses allow the formation of cracks with ductile fracture and the chip separation.

Figure 5 presents a detail of the chip root formation from figure 4 with the FEM mesh applied. It is possible to observe the material separation that occurs near the cutting edge, to form the chip, and identify elements with tensile and compressive stresses in the region.

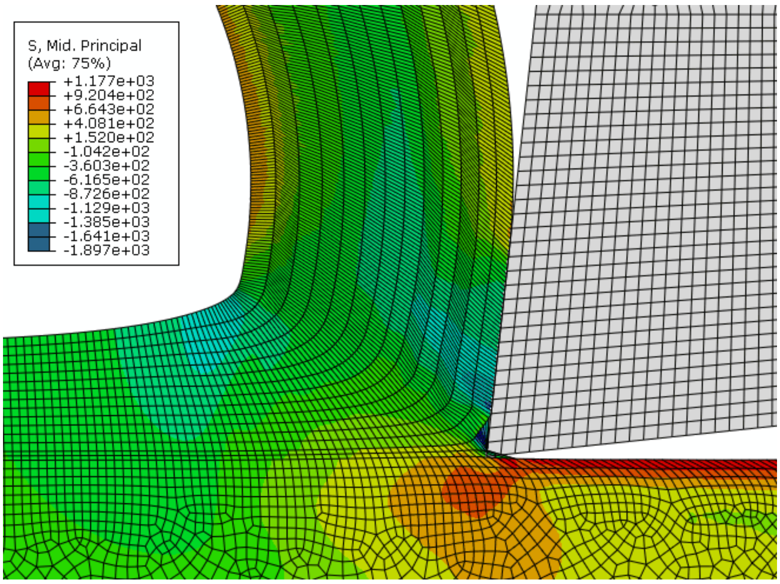

Figure 5. Hydrostatic stress with the FEM mesh [MPa]. vc= 79 m/min, f = 0.1mm/rev and ap = 2 mm.

3.2 Results from the chip root observation

In order to evaluate the possible occurrence of cracks during the chip formation some machining tests were carried out using the quick stop device. Figure 6 shows the results obtained with a shaft made of AISI 304 with vc = 50 m/min, f= 0.1mm/rev, and ap = 1mm.

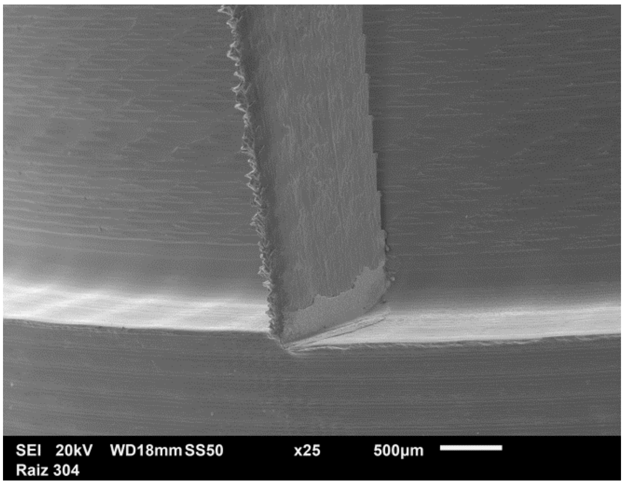

(a)

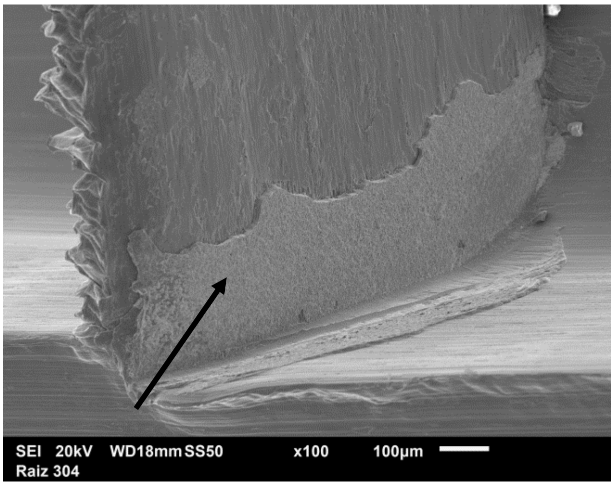

(b)

Figure 6. SEM, chip roots AISI 304. vc = 50 m/min, f = 0.1mm/rev, and ap = 1mm.

It is possible to check a layer of adhered material near the chip root, indicated by the arrow in Fig. 6(b). This material comes from the formation of build up edge between the chip and the tool, and makes it difficult to verify the presence of cracks in the chip root.

Austenitic stainless steels are difficult to cut materials. The high work hardening and low thermal conductivity are responsible for their poor machinability. In addition, these materials usually bond to the rake face of the tool and forms build up edge, especially in low cutting speeds, as observed in Fig. 6.

Several machining tests were carried out with different cutting speeds using the quick stop device, in this case with a tube made of AISI 303 stainless steel. Figure 7 shows a sample of a chip obtained. The cutting parameters used was vc= 50 m/min, f = 0,1mm/rot, and ap = 1mm.

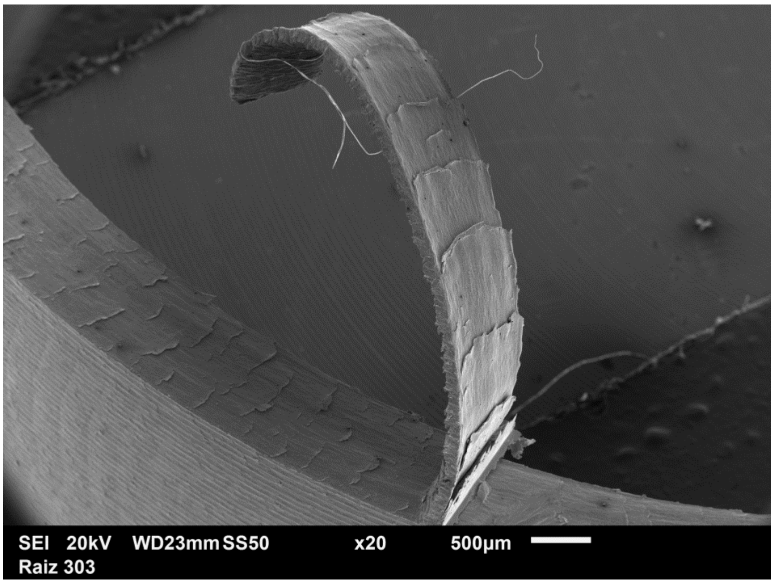

Figure 7. SEM, chip formation. vc = 50 m/min, f = 0.1mm/rev, and ap = 1mm.

Figure 8 shows a magnification of the chip root from Fig. 7. It is possible to observe the materials that were adhered in the cutting edge and rake face of the tool and formed a build-up edge. The arrows in Fig. 8(a) and Fig. 8(b) indicates possible regions with ductile fracture ahead of the cutting edge.

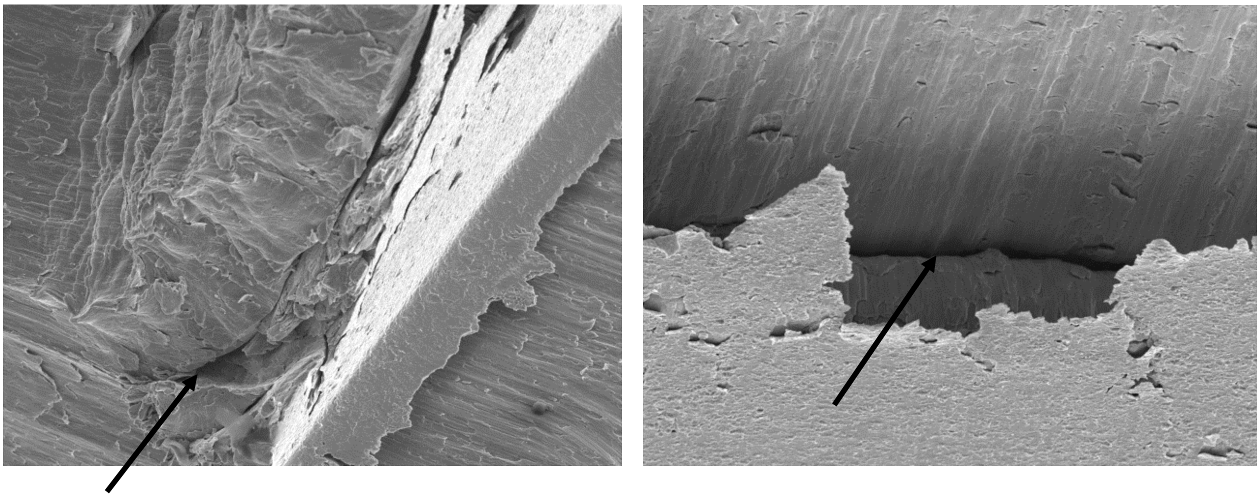

Figure 8. Chip roots. (a) side view detail; (b) front view detail. vc = 50 m/min, f = 0.1mm/rev, and ap = 1mm.

The machining tests revealed the difficulty to obtain a chip root specimen using the quick stop device that allows the visualization of cracks during the chip formation. The results obtained suggest the existence of fracture in the chip root region. Otherwise, it is required to perform other experiments, with different cutting speeds and cutting tools, to avoid the formation of build up edge, in order to obtain new evidences to prove the formation of ductile fracture in the chip root region during machining of austenitic stainless steels.

4. CONCLUSIONS

The results obtained in the machining simulations showed a favorable condition to the formation of chip fracture due to the occurrence of tensile stresses in the chip root, near the tool tip. Experimental procedures performed with a quick stop device during machining showed possible regions in the chip root where ductile fracture occurs. This result is in accordance with the theory that during machining a localized fracture in chip formation leads to material separation and forms a new surface.

The FEM model developed considered the material separation with damage and ductile fracture obtained good results and is considered appropriate to represent and simulate the machining process.

5. ACKNOWLEDGEMENTS

The authors are grateful to IFSC, CNPq and FAPESP, for their financial support.

6. REFERENCES

Agmell, M., Ahadi, A., Stahl,.E., 2011. “A numerical and experimental investigation of the deformation zones and the corresponding cutting forces in orthogonal cutting”. *Advanced Materials Research*, vol. 223, p.152-161.

American Society for Metals. ASM Handbook, 2005. *Properties and selection: Irons, Steels, and High Performance Alloys*. 10 ed, vol.1, 1618p.

Arrazola, P.J., Ozel, T., Umbrello, D., Davies, M., Jawahir, I.S., 2013. “Recent advances in modelling of metal machining processes”. *CIRP Annals Manufacturing Technology*, vol. 62, p. 695–718.

Astakov, V.P., 2006. *Tribology of metal cutting*. Elsevier Science, 1ed, 292p.

Atkins, A.G., 2003. “Modelling metal cutting using modern ductile fracture mechanics: quantitative explanations for some longstanding problems”. *International Journal of Mechanical Sciences*, vol. 45, p. 373–396.

Chagas, G.M.P., Machado, I.F.,2015. “Numerical model of machining considering the effect of MnS inclusions in an austenitic stainless steel”. *Procedia CIRP*. vol.31, p. 533 – 538.

Chern, G. L., 2005, “Development of a new and simple quick-stop device for the study on chip formation.” *International Journal of Machine Tools & Manufacture*, vol. 45, p.789-794.

Childs, T.H.C., 2010. “Surface energy, cutting edge radius and material flow stress size effects in continuous chip formation of metals”. *CIRP Journal of Manufacturing Science and Technology*, vol.3, p.27-39.

Johnson, G. R., Cook, W. H., 1983. “A constitutive model and data for metals subjected to various strains, high strain rates, and high temperatures”. *Proceedings of the Seventh International Symposium on Ballistics*. p. 541-547.

Lalwani, D.I., Mehta, N.K., Jain, P.K., 2009. “Extension of Oxley’s predictive machining theory for Johnson and Cook flow stress model. *Journal of Materials Processing Technology*, vol.209, p.5305-5312.

Lee, S., Barthelat, F., Hutchinson, JW., Espinosa, H.D., 2006. “Dynamic failure of metallic pyramidal truss core materials - Experiments and modeling”. *International Journal of Plasticity*, vol. 22, p. 2118–2145.

Lindgren, L.E., Svoboda, A., Wedberg, D., Lundblad, M., 2016, “Towards predictive simulations of machining”, *Comptes Rendus Mecanique*, vol. 344, p. 284-295.

Madhavan, V., Chandrasekar,S., Farris, T.N., 2000. “Machining as a wedge indentation”. *Transactions of the ASME*. vol. 67, p.128 - 139.

Matweb Material property data. <http://www.matweb.com>. Access in: 12 jan. 2017.

Ozel, T., 2006. “The influence of friction models on finite element simulations of machining”. *International Journal of Machine Tools & Manufacture*. vol. 46, p.518–530.

Rosa, P., Martins, P., Atkins, A.G., 2007. “ Revisiting the fundamentals of metal cutting by means of finite elements and ductile fractures mechanics”. *International Journal of Machine Tools & Manufacture*. 47, p. 607-617.

Shaw, M. C. 2005. *Metal cutting principles*. New York: Oxford University Press, 2 ed., 651p.

Simulia. 2012. *Abaqus analysis user manual* . 6.12. v.3: material.

Souza L. *Evaluation of cutting parameters and heat treatments in the turning process of three austenitic stainless steels*. Master dissertation. Universidade de São Paulo. 2006. (In Portuguese).

Subbiah, S.; Melkote,S.N., 2007. “ Evaluation of Atkins’ model of ductile machining including the material separation component”. *Journal of Materials Processing Technology*, vol. 182, p.398–404.

Subbiah, S.; Melkote,S.N., 2008. “ Effect of finite edge radius on ductile fracture ahead of the cutting tool edge in micro cutting of Al2024-T3”. *Materials Science and Engineering A*. vol. 474, p.283-300.

7. RESPONSIBILITY NOTICE

The authors are the only responsible for the printed material included in this paper.